We thank the referee for the insightful comments and suggestions, which give us new perspectives to describe our work and greatly helped to improve the significance of the paper. Our answers are listed in the following in red, after the referee's comments, which are in black. The modifications in the text are marked in yellow.

Reviewer #1

This paper describes an improved direct measurement system of the photochemical ozone production rate ($P(O_3)$). The authors also performed a field observation of $P(O_3)$ and evaluated the instrument and observation results using a detailed box model simulation.

O_3 pollution is a crucial problem for atmospheric environment, and a behavior of O_3 is very difficult, so direct measurements of $P(O_3)$ such as this research are very important and valuable. However, this paper has major concerns about the evaluation by the box model simulation. So, I cannot recommend this paper to be published in Atmospheric Chemistry and Physics in the present form. The authors should resolve the concerns by re-evaluation of the box model simulation or other ways.

Thank you very much for providing useful suggestions. We agree with the reviewer that some of the modeling results in the reference chamber were beyond our expectation. Therefore, we have re-evaluated and carefully checked each step of the box model simulations described in Sect. 3.2, but no error has been found so far. To make the modeling results clearer, we added the budgets of OH, HO_2, RO_2, and NO_3 during the 3rd-stage 4-min model simulation in the reaction and reference chambers. The main purposes of performing the box model simulation in this study are as follows: ① how to determine the photolysis frequencies for $P(O_3)_{net}$ modeling in ambient air by comparing the modeling results with the measured results, and ② provide a comprehensive understanding of the radical budgets in the reaction and reference chambers. The reactions occurring in the reference chamber are much more complex than those in the reaction chamber, and the results are also different when we use different J value determination methods (labeled as method I and method II). However, the biases of the modeled $P(O_3)_{net}$ caused by the interferences in the reference chamber were 13.9 % and 22.3 % in method I and method II, respectively, which ensures that the measured $P(O_3)_{net}$ by the NPOPR detection system should be regarded as the lower limit values of the real $P(O_3)_{net}$ in the atmosphere. We made some additional box model simulations and answered the reviewer's questions point by point as follows:

Major comments:

- The results of the box model simulation

I suspect such high concentrations of NO_3 in the reference chamber. First, the value of JNO_3 in the reference chamber is about 90% of that in the reaction chamber, which is sufficiently high. Second, the rate constant of the reaction of NO_3 with NO is sufficiently large and the lifetime of NO_3 (at 298 K) is 1.6 s and very short in the presence of NO of 1 ppbv. There might be high concentrations of NO_3 if there are very large sources of NO_3, but in that case, the authors should mention the evidence. I think the NO_2 + O_3 reaction cannot be a large source of NO_3. I'm not sure about N_2O_5, but it is unlikely that there could be high concentrations of N_2O_5 under the temperature during the observation period.

To explore the reason for such a high concentration of NO_3 in the reference chamber, we modeled the production and destruction pathways of NO_3 in the reaction and reference chambers (as shown in Fig. S19 for method I and method II). First, we found that even when the $J(NO_3)$ values were sufficiently large (which were 90% and 100% of that in the reaction chamber for method I and method II, respectively), which led to a high NO_3 photolysis reaction in the reference chamber, the NO_3 concentrations were still sufficiently high due to the high production rates of NO_3 at the same time (the main production pathway of NO_3 is the NO_2+O_3 reaction, followed by N_2O_5 decomposition). Second, the NO concentrations were large in the 1st minute, which consumes NO_3 very quickly, but as there were continuous NO_3 sources, the net NO_3 production rates ($P(NO_3)_{net}$) were positive, which caused the NO_3 concentration to continue to increase (as shown in Figs. 8d and S20).

The main difference of NO_3 production in the reference chamber compared to that in the reaction chamber is the much higher N_2O_5 decomposition. A proposed mechanism for the decomposition of N_2O_5 is as follows (Kotz et al., 2019):

$$N_2O_5 \xrightarrow{k1} NO_2+NO_3 \qquad \text{step 1 (slow)}$$

$$NO_2+NO_3 \xrightarrow{k2} NO_2 + O_2 + NO \qquad \text{step 2 (fast)}$$

$$NO+N_2O_5 \xrightarrow{k3} 3NO_2 \qquad \text{step 3 (fast)}$$

We proposed that due to the much higher NO_2 concentrations in the reference chamber than in the reaction chamber, NO_3 is consumed to produce NO in step 2, which accelerates step 1 and benefits step 3, thus increasing the steady-state concentration of NO_3. This is also demonstrated by the increased N_2O_5 decomposition and NO_2 concentrations along with the increased NO_2+NO_3 reaction (as shown in Figs. 8-9 and S18-S19). Therefore, the high NO_3 concentrations in the reference chamber were mainly due to the high NO_2 concentrations. On the other hand, although the NO_2+NO_3 reaction was also one of the dominant NO_3 destruction pathways, NO_3 consumed by the reaction of

NO_2+NO_3 was significantly smaller than NO3 produced by the reaction of NO2+O3 (as shown in Figs. 9 and S19).

We added the related discussion for method I in pages 24-25, lines 551-567 in the modified manuscript:

"Due to sufficiently high $J(NO_3)$ (~ 90% of that in the reaction chamber) and NO_2 concentrations in the reference chamber, the NO_3 photolysis and NO_2+NO_3 reaction consumed NO_3 in the reference chamber, but the NO_3 concentrations were still sufficiently high due to high production rates of NO_3 at the same time. The main NO_3 source in the reference chamber was the NO_2+O_3 reaction, followed by N_2O_5 decomposition. The NO concentrations were relatively high in the 1st minute and consumed NO_3 very quickly, but due to continuous NO_3 sources, the net NO_3 production rates ($P(NO_3)_{net}$) were positive (as shown in Fig. 9), which caused the NO_3 concentration to continue to increase (as shown in Fig. 8d). The main difference in NO_3 production in the reference chamber compared to that in the reaction chamber was the much higher N_2O_5 decomposition, which was mainly due to the high NO_2 concentrations in the reference chamber. On the other hand, although the NO+NO_3 reaction was also one of the dominant NO_3 destruction pathways, NO_3 consumed by the NO+NO_3 reaction was significantly smaller than NO_3 produced by the NO_2+O_3 reaction. Furthermore, in order to check if the NO_3+VOCs reactions exists, we extracted all the P(ROx) pathways related to NO_3+VOCs reactions during the 3rd-stage 4-min model simulation in the reaction and reference chambers in method I, as shown in Fig. S20. We found that the NO_3+VOCs reactions are mostly related to the OVOCs (i.e. 6-Ethyl-m-cresol and 3-Ethyl-6-methylbenzene-1,2-diol) in Fig. S21. The production and destruction rates of ROx are shown in Fig. S20."

And added the related discussion for method II in page 25, lines 330-343 in the modified supplementary materials:

Due to sufficiently high $J(NO_3)$ (~ 100 % of that in the reaction chamber) and NO_2 concentrations in the reference chamber, the NO_3 photolysis and NO_2+NO_3 reaction consumed NO_3 in the reference chamber, but the NO_3 concentrations were still high due to high production rates of NO_3 at the same time. Similar with the results obtained from method I as described in the main manuscript, for method II, the main NO_3 source in the reference chamber was the NO_2+O_3 reaction, followed by N_2O_5 decomposition. The NO concentrations were relatively high in the 1st minute and consumed NO_3 very quickly, but due to continuous NO_3 sources, the net NO_3 production rates ($P(NO_3)_{net}$) were positive (as shown in Fig.

S19b4), which caused the NO_3 concentration to continue to increase (as shown in Fig. S18d). The main difference in NO_3 production in the reference chamber compared to that in the reaction chamber was the much higher N_2O_5 decomposition, which was mainly due to the high NO_2 concentrations in the reference chamber. On the other hand, although the NO+NO_3 reaction was also one of the dominant NO_3 destruction pathways, NO_3 consumed by the NO+NO_3 reaction was significantly smaller than NO_3 produced by the NO_2+O_3 reaction. The integrated production and destruction rates of ROx are shown in Fig. S20.

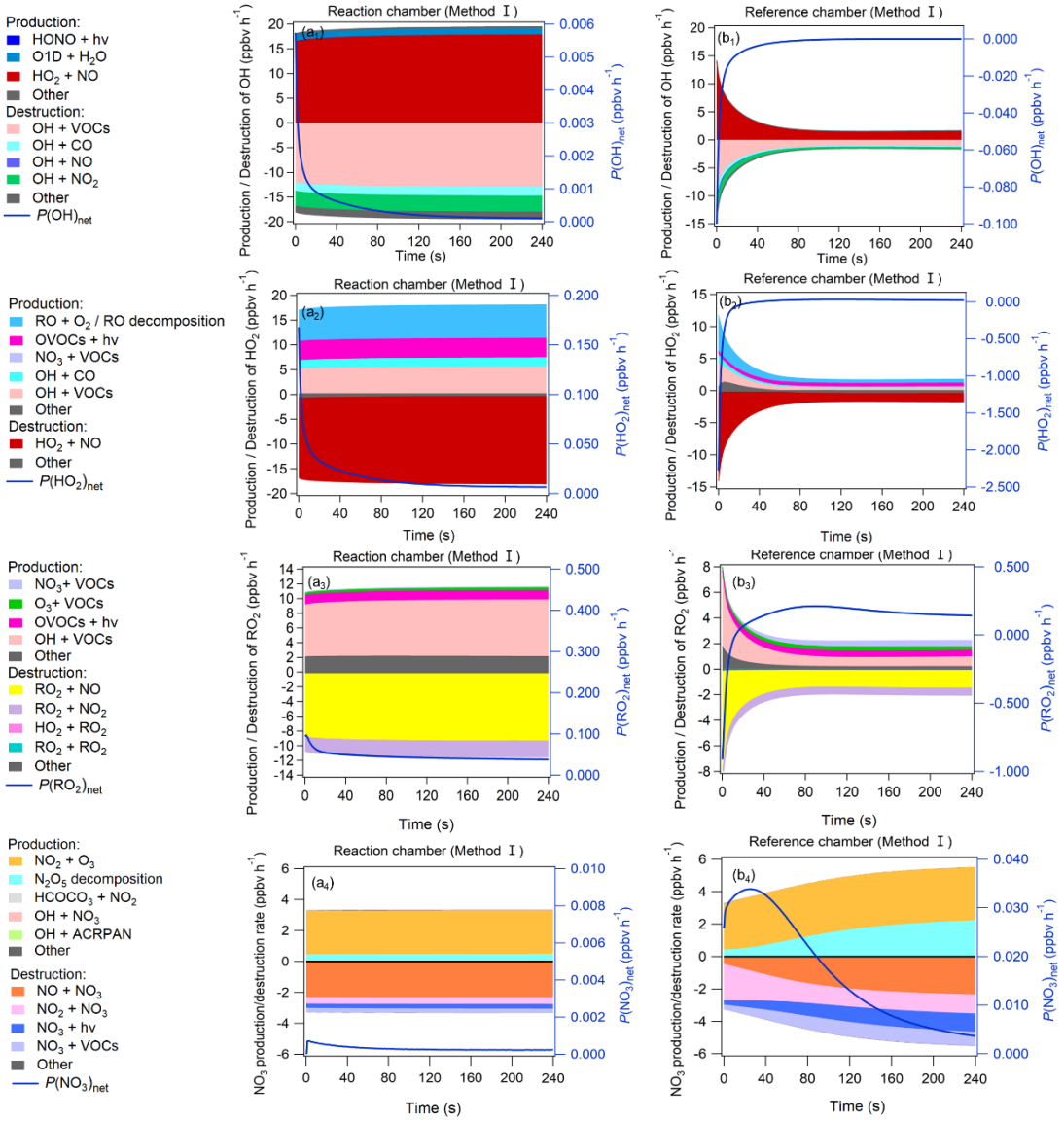

Figure 9: Production and destruction pathways of OH (a_1-b_1), HO_2 (a_2-b_2), RO_2 (a_3-b_3), and NO_3 (a_4-b_4) during the 3rd-stage 4-min model simulation in the reaction and reference chambers in method I. The related contents for method II (c)-(d) are shown in Fig. S19 in the supplementary materials.

And added Fig. S19 in the modified supplementary materials:

"Due to sufficiently high $J(NO_3)$ (~ 100 % of that in the reaction chamber) and NO_2 concentrations in the reference chamber, the NO_3 photolysis and NO_2+NO_3 reaction consumed NO_3 in the reference chamber, but the NO_3 concentrations were still high due to high production rates of NO_3 at the same time. Similar with the results obtained from method I as described in the main manuscript, for method II, the main NO_3 source in the reference chamber was the NO_2+O_3 reaction, followed by N_2O_5 decomposition. The NO concentrations were relatively high in the 1st minute and consumed NO_3 very quickly, but due to continuous NO_3 sources, the net NO_3 production rates ($P(NO_3)_{net}$) were positive (as shown in Fig. S19b4), which caused the NO_3 concentration to continue to increase (as shown in Fig. S18d). The main difference in NO_3 production in the reference chamber compared to that in the reaction chamber was the much higher N_2O_5 decomposition, which was mainly due to the high NO_2 concentrations in the reference chamber. On the other hand, although the NO+NO_3 reaction was also one of the dominant NO_3 destruction pathways, NO_3 consumed by the NO+NO_3 reaction was significantly smaller than NO_3 produced by the NO_2+O_3 reaction."

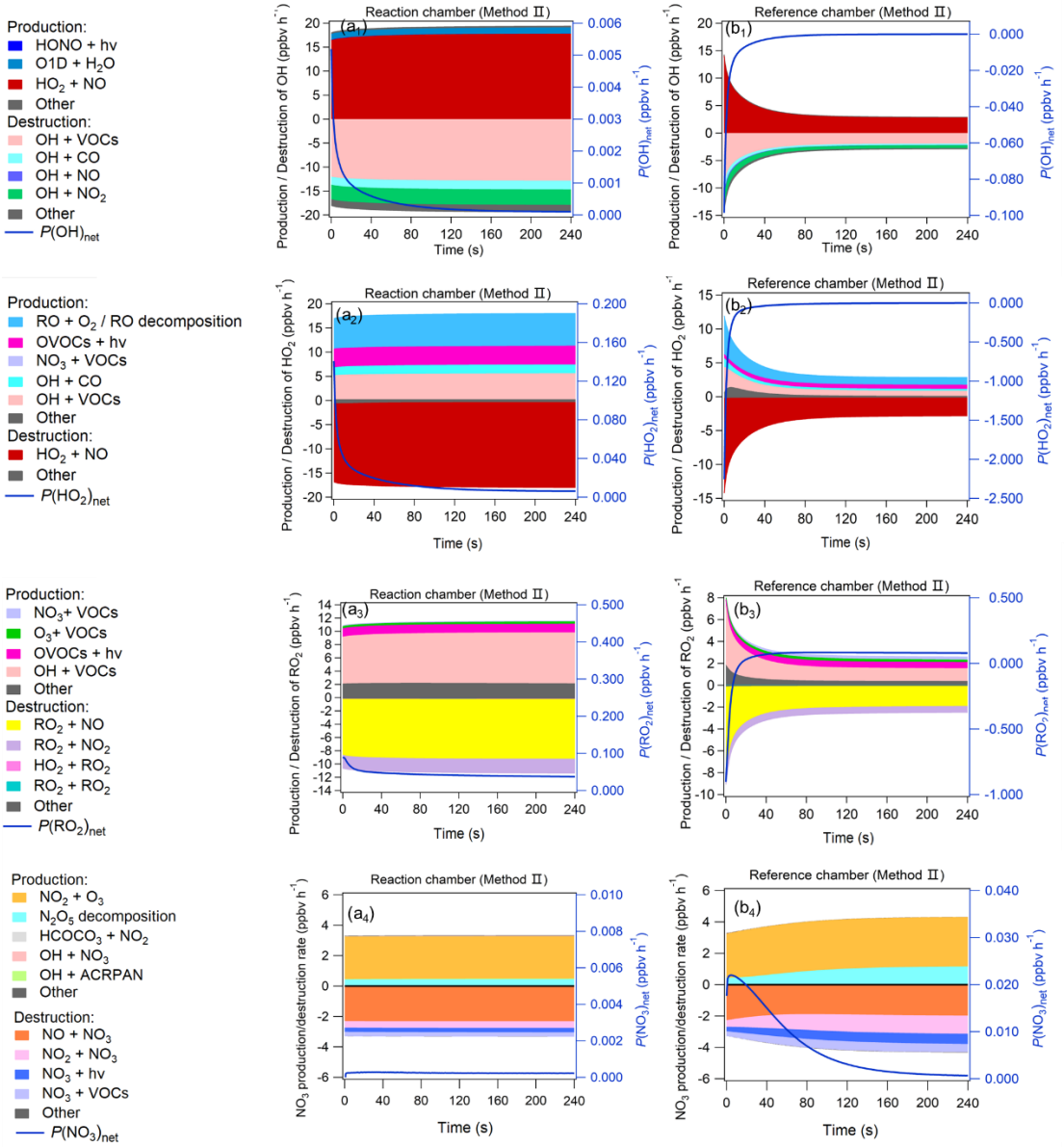

Figure S19: Production and destruction pathways of OH(a_1-b_1), HO_2(a_2-b_2), RO_2(a_3-b_3), and NO_3(a_4-b_4) during the 3rd-stag 4-min model simulation in the reaction and reference chambers in method II (c)-(d).

On the other hand, I also suspect the reaction of NO_3 with VOCs as a major source of RO_2 in the reference chamber. The rate constants of the reactions of NO_3 with VOCs are not so large, and it is questionable that NO_3 and RO_2 concentrations change in minutes by the reactions of NO_3 with VOCs unless there are extremely high concentrations of VOCs.

The reviewer is correct. We actually described it incorrectly here, and we apologize for this mistake. The major RO_2 sources in the reference chamber were OH+VOC oxidation, followed by OVOC photolysis (i.e., $C_3H_4O_2$, $C_2H_2O_2$, $C_4H_6O_2$, etc.) and O_3+VOC reactions. To better understand the radical chemistry, we included the

production and destruction pathways of OH, HO_2, RO_2, and NO_3 during the 3rd-stage 4-min model simulation in the reaction and reference chambers in Figs. 9 and S19 (as shown above) and moved the production and destruction pathways of ROx to Fig. S20.

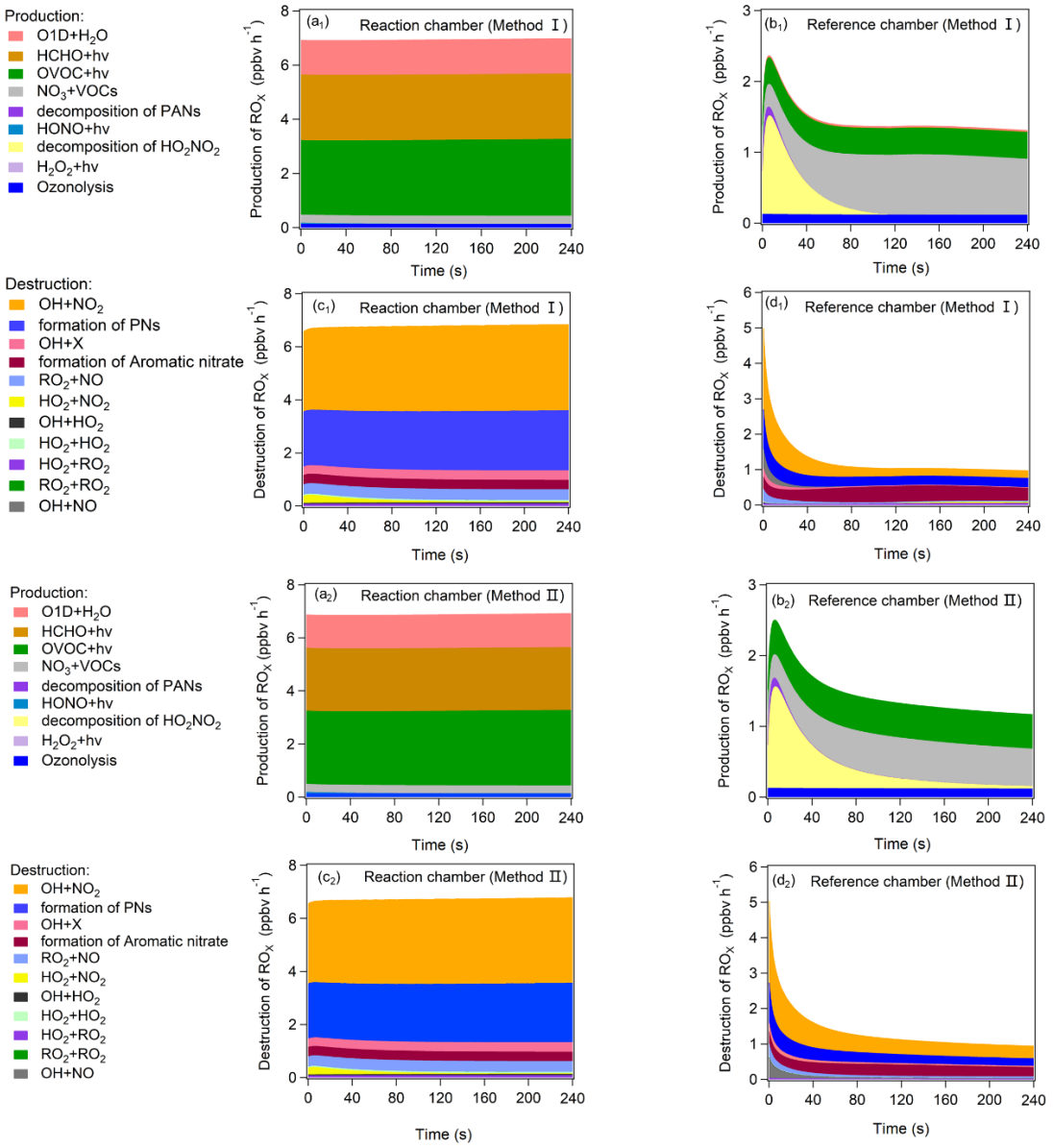

Figure S20: Production and destruction pathways of ROX during the 3rd-stage 4-min model simulation in the reaction and reference chambers. (PAN: Peroxyacetyl Nitrate; PNs: formations of all peroxynitrate (including $CH_3O_2NO_2$ and PAN; X: PAN and the net loss of OH+NO to form HONO (usually small)).

Accordingly, we modified the related description in page 24, lines 542-552 in the modified manuscript:

"OH, HO_2, RO_2, and NO_3 concentrations greatly impact the O_3 production and destruction rate. To better understand the factors that drive the OH, HO_2, RO_2, and NO_3 concentration changes, we have added their production and destruction pathways in Fig. 9. We found that the decrease in HO_2 and RO_2 concentrations in the reference chamber in the 1st half minute was mainly due to NO titration effects, as high NO mixing ratios existed during the 1st half minute. The increase in HO_2 concentrations afterward was largely attributable to RO+O_2 reaction/RO decomposition, OH+CO/VOCs reaction, OVOCs photolysis (i.e., $C_3H_4O_2$, $C_2H_2O_2$, $C_4H_6O_2$), and NO_3+VOCs reaction, and the increase in RO_2 concentrations afterward were largely attributable to OH+VOCs oxidation, OVOCs photolysis and O_3+VOCs reaction. The main OH sources in the reference chamber were both HO_2+NO in method I and method II."

And in pages 24-25, lines 318-329 in the modified supplementary materials:

"OH, HO_2, RO_2, and NO_3 concentrations greatly impact the O_3 production and destruction rate. To better understand the factors that drive the OH, HO_2, RO_2, and NO_3 concentration changes in method II, we have added their production and destruction pathways in Fig. S19. We found that the decrease in HO_2 and RO_2 concentrations in the reference chamber in the 1st half minute was mainly due to NO titration effects, as high NO mixing ratios existed during the 1st half minute. The HO_2 and RO_2 concentrations were became stable afterwards, the main production pathway for HO_2 was RO+O_2 reaction/RO decomposition, followed by OH+ VOCs reaction, OVOCs photolysis (i.e., $C_3H_4O_2$, $C_2H_2O_2$, $C_4H_6O_2$), and NO_3+VOCs reaction; while the main production pathway for RO_2 was OH+ VOCs reaction, followed by OVOCs photolysis (i.e., $C_3H_4O_2$, $C_2H_2O_2$, $C_4H_6O_2$), OH+CO, NO_3+VOCs reaction, etc.; the main destruction pathways for HO_2 and RO_2 were HO_2+NO and RO_2+NO, respectively. The main OH production and destruction pathways in the reference chamber was HO_2+NO reaction and OH+ VOCs reaction, respectively."

Furthermore, in order to check if the NO_3+VOCs reactions exists, we extracted all the *P*(ROx) pathways related to NO_3+VOCs reactions during the 3rd-stage 4-min model simulation in the reaction and reference chambers in method I, as shown in Fig. S20. We found that the NO_3+VOCs reactions are mostly related to the OVOCs (i.e. 6-Ethyl-m-cresol and 3-Ethyl-6-methylbenzene-1,2-diol), as shown in Fig. S21.

The related explanations are added in page 25, line 562-567 in the modified manuscript:

"Furthermore, in order to check if the NO_3+VOCs reactions exists, we extracted all the *P*(ROx) pathways related to NO_3+VOCs reactions during the 3rd-stage 4-min model simulation in the reaction and reference chambers in method I, as shown in Fig. S20. We found that the NO_3+VOCs reactions are mostly related to the OVOCs (i.e. 6-Ethyl-m-cresol and 3-Ethyl-6-methylbenzene-1,2-diol) in Fig. S21. The production and destruction rates of ROx are shown in Fig. S20."

And in page 27, lines 354-357 in the modified supplementary materials:

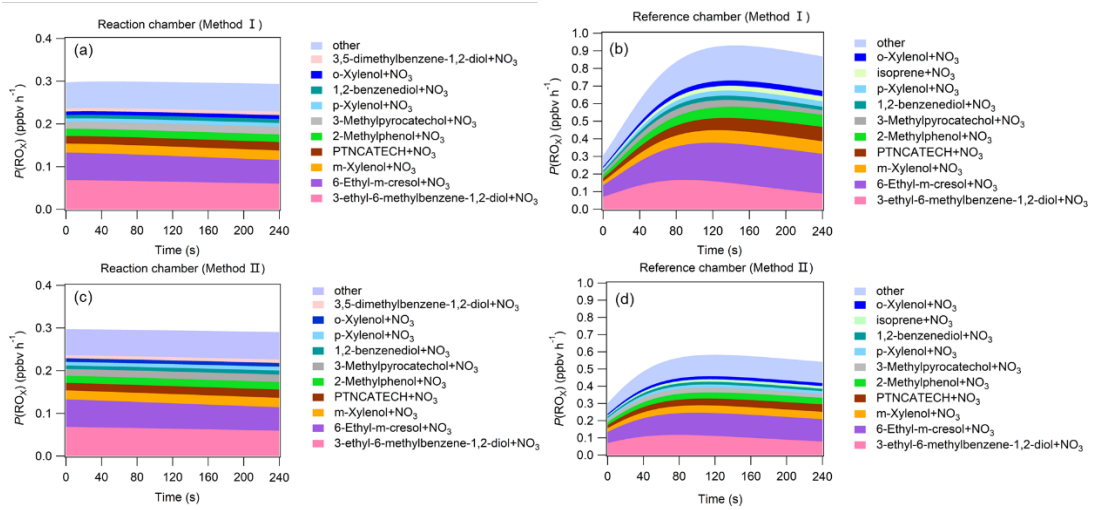

Figure S21: The *P*(ROx) pathways related to NO_3+VOCs reactions during the 3rd-stage 4-minute model simulation in the reaction and reference chambers in method I (a)-(b) and method II (c)-(d).

For Figs. 9(b) and S10(b), photodissociation of OVOCs is a significant part of ROx sources in the reference chamber. Why such a large fraction in the absence of UV? The authors should mention the evidence.

The reference chamber was covered by a UV protection Ultem film (SH2CLAR, 3M, Japan) to block the sunlight with the wavelengths < 390 nm, so the film has the transmission of lights > 390 nm, thus the photolysis frequencies of some species still existed, as shown in Tables S7 and S13. Therefore, we still observed OVOCs photodissociation in the reference chamber., i.e., $C_3H_4O_2$, $C_2H_2O_2$, $C_4H_6O_2$ and $C_4H_4O_4$, etc. According to MCMv3.3.1, there are in total 979 OVOCs species photolysis in the reference chamber, some of which are listed as follows:

Photolysis reactions from IUPAC Task Group on Atmospheric Chemical Kinetic Data Evaluation (http://iupac. pole-ether.fr/):

1. $C_3H_4O_2$ (Methylglyoxal) $\xrightarrow{h\nu: 225\text{-}410\ nm}$ $CH_3CO_3 + CO + H_2O$ IUPAC (2006)

2. ①$C_2H_2O_2$ (Glyoxal) $\xrightarrow{h\nu: 230.5\text{-}462.0\ nm}$ $CO + CO + H_2$ IUPAC(2006)

②$C_2H_2O_2$(Glyoxal) $\xrightarrow{h\nu: 230.5\text{-}462.0\ nm}$ $CO + CO + HO_2 + HO_2$ IUPAC(2006)

③$C_2H_2O_2$ (Glyoxal) $\xrightarrow{h\nu: 230.5\text{-}462.0\ nm}$ HCHO + CO IUPAC(2006)

3. $C_4H_6O_2$ (Biacetyl) $\xrightarrow{h\nu: 206\text{-}493\ nm}$ $CH_3CO_3 + CH_3CO_3$ IUPAC(2011)

4. $C_4H_6O_2$ (Ethylglyoxal) $\xrightarrow{h\nu: 225\text{-}410\ nm}$ $C_2H_5CO_3 + CO + HO_2$ IUPAC(2006)

We added the evidence in page 24, lines 546-550 in the modified manuscript:

"The increase in HO_2 concentrations afterward was largely attributable to $RO+O_2$ reaction/RO decomposition, OH+CO/VOCs reaction, OVOCs photolysis (i.e., $C_3H_4O_2$, $C_2H_2O_2$, $C_4H_6O_2$), and NO_3+VOCs reaction, and the increase in RO_2 concentrations afterward were largely attributable to OH+VOCs oxidation, OVOCs photolysis and O_3+VOCs reaction."

I entertain doubts about the results of the present box model simulation. I think the authors should revalidate the appropriateness of the model thoroughly.

We have re-evaluated the model simulations and added more model simulations to explain some abnormal phenomena in the reference chamber, such as the production and destruction pathways of OH, HO_2, RO_2, and NO_3 during the 3rd-stage 4-min model simulation in the reaction and reference chambers, the NO_3+VOC reactions, etc. We found that the radicals and gas species in the reaction chamber of the NPOPR detection system were similar to those in the ambient air, while these radicals also unexpectedly existed in the reference chamber. This was mainly because the UV protection film used by the reference chamber did not completely filter out sunlight, which led to the low transmittance of light ranging from 390 nm to 790 nm. We evaluated the interference of the unexpected reactions in the reference chambers and found that the biases of the modeled $P(O_3)_{net}$ caused by this interference using method I and method II were 13.9 % and 22.3 %, respectively; therefore, we noted that ozone photochemical production still existed in the reference chamber, and the measured $P(O_3)_{net}$ by the NPOPR system should be regarded as the lower limit values, as described in page 29, in lines 650-660 in the modified manuscript:

"In conclusion, modeling tests demonstrated that the radicals and gas species in the reaction

chamber of the NPOPR detection system were similar to those in genuine ambient air, while these radicals also unexpectedly existed in the reference chamber. This was mainly because the UV protection film used by the reference chamber did not completely filter out sunlight, which led to the low transmittance of light ranging from 390 nm to 790 nm. The $P(O_3)_{net}$ biases caused by this interference modeled in method I and method II were 13.9 % and 22.3 %, respectively, which ensured that the measured $P(O_3)_{net}$ by the NPOPR detection system should be regarded as the lower limit values of real $P(O_3)_{net}$ in the atmosphere. We recommend that the *J* values obtained from method I should be used in the model simulation, which can better explain the photochemical formation of O_3 in the actual atmosphere, but if direct *J* value measurements cannot be achieved during field observations, the *J* values obtained from method II would also be acceptable in modeling studies."

Answers to all of the reviewer's concerns are listed in the following:

- Measurements of NOx using a chemiluminescence NOx monitor.

Did the authors use a commercially available chemiluminescence NOx monitor without further modification? If so, accuracy of NO_2 and NOx concentrations would be low because NOz such as HNO_3 and PANs interfere observed values of NO_2 and NOx. I think this interference could affect discussion in this paper, so the authors should evaluate the interference quantitatively. In the fresh air masses, the interference by descendent pollutants of NOx such as HNO_3 and PANs might be small, but that by HONO could be large instead.

Yes, we used a commercially available chemiluminescence NOx monitor without further modification. To investigate the interference of HNO_3 and PANs, we added an evaluation of the effect of the NO_2 measurement bias of the chemiluminescence NOx monitor on $P(O_3)_{net}$. We compared the NO_2 measured by the chemiluminescence NOx monitor with that measured by the CAPS (which is regarded as the trustable NO_2 measurement technique without chemical interference) and revealed that a 5% bias could be caused by the chemiluminescence NOx monitor (will be published elsewhere). Therefore, we simulated $P(O_3)_{net}$ by reducing and increasing the mixing ratios of NO_2 by 5 % to check the interference caused by using the chemiluminescence NOx monitor to $P(O_3)_{net}$. The results show that increasing and decreasing NO_2 by 5 % resulted in a decrease in $P(O_3)_{net}$ by 1.64 % and 3.68 %, respectively. We added this explanation in the modified manuscript in pages 29-30, lines 661-671:"

"Furthermore, because the NO_2 data used here were measured by a commercially available chemiluminescence NOx monitor, the NO_2 and NOx mixing ratios would be overestimated due to NOz

interference (i.e., HNO_3, PANs, HONO, etc.) (Dunlea et al., 2007). According to our test, the chemiluminescence technique could bias NO_2 by 5 % compared to the CAPS technique, which is regarded as a trustworthy NO_2 measurement technique without chemical interference. Therefore, we simulated the interference of NO_2 measured by a chemiluminescence NOx monitor in method I as follows: reducing and increasing the ambient NO_2 mixing ratios by 5 % in the 3rd-stage 4-min simulation in the reaction and reference chambers. The results show that increasing and decreasing NO_2 by 5 % resulted in a decrease in $P(O_3)_{net}$ by 1.64 % and 3.68 %, respectively (as shown in Fig. S23), which is much smaller than the bias caused by $P(O_3)_{net}$ in the reference chambers (which were 13.9 % and 22.3 % for method I and method II, respectively)."

And added Fig. S23 in the modified supplementary materials:

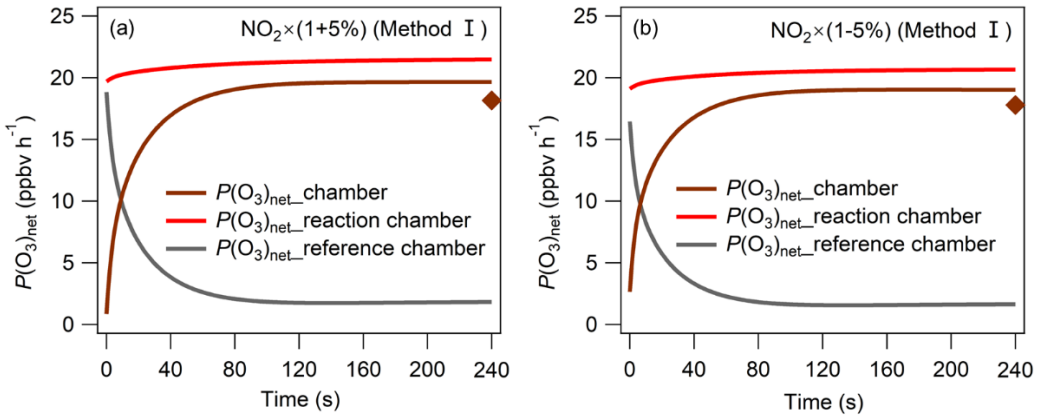

Figure S23: $P(O_3)_{net}$ changing in the reaction and reference chambers in method I with ± 5 % of measured NO_2.

Other minor comments:

Some mathematical formulae: The authors should use italic and roman letters correctly.

We have changed the font of the formula to italic and roman letters in the modified manuscript (in lines 56-57, 167, 292, 322, 364, 382, 395-396 and 481-483) and supplementary materials (in line 26, 28, 53-54, 206, 217, 235, 286 and Table S12).

L65: at 424 nm → at < 424 nm

We revised it in lines 65-66 in the modified manuscript: "The specific process of the photochemical reaction is the photolysis of NO_2 at < 420 nm to generate $O(^3P)$ atoms, thereby promoting the formation of O_3 (Sadanaga et al., 2017)."

L72: are proportional to → affect?

We wanted to express that the surface deposition and advection of O_3 **are proportional to** ambient O_3 mixing ratios, [O_3], which is mainly generated by local photochemistry (Carzorla et al., 2010). We have added the reference in line 73 in the modified manuscript.

Fig. 1: Why do the authors use critical orifices instead of mass flow controllers? Is the temperature of orifices controlled to keep a constant flow rate?

According to our tests, using critical orifices will make the sampling air flow rate in the reaction and reference chambers more stable than using mass flow controllers. We ensured that the air flow rates during the measurement period were constant in the reaction and reference chambers by checking the air flow rates every day during the campaign. Furthermore, the temperature of the orifices did not increase during the sampling time; thus, we assumed that the temperature of the orifices did not affect the air flow rate.

Fig. 1: Are inner walls of the reaction and reference chambers coated with Teflon? If so, please indicate the kind of the Teflon coat.

We did not coat the inner walls of the reaction and reference chambers with Teflon. The reasons are listed as follows: 1) Sadanaga et al. (2017) reported 8–10% dark losses of O_3 on uncoated quartz surfaces for a residence time of 21 min in the chambers, which is consistent with the reported dark loss of less than 5% for O_3-conditioned flow chambers and a residence time of 4.5 min in Sklaveniti et al. (2018). Sadanaga et al. (2017) indicated that the values of $[NO_2]_{out}$ were in agreement with $[NO_2]_{in}$ within one standard deviation under both dry (0%) and humidified (80%) conditions. The NO_2 loss is lower than 5% in both flow chambers and is close to 3% on average in Sklaveniti et al. (2018) under dark conditions. In our study, the wall losses of NO_2 were lower than 4% and 2% in the reaction and reference chambers, respectively, and the wall losses of O_3 were both lower than 3% in the reaction and reference chambers, as shown in Tables S2 and S3; thus, we assumed this would not cause much bias in our measurement results under dark conditions. 2) Sklaveniti et al. (2018) thought Teflon coating seemed to remove or reduce the photolytic loss of ozone to a negligible level on their instrument because they thought the instrument design reported by Sadanaga et al. (2017) did not seem to be significantly impacted by a photolytic loss of ozone on the quartz flow chambers whose inner surface was coated with Teflon. In

Sadanaga et al. (2017), wall losses of O_3 were found to be approximately 10% for both chambers without clear Teflon coating, but wall losses decreased to less than 1.5% when the chambers were coated with Teflon. In our study, we calibrated photolytic O_3 losses by performing a set of laboratory and ambient experiments (see sec. S2, pages 18-20 lines 207-237 in the supplementary materials), the results after photolytic O_3 loss correction compensated for the photolytic O_3 loss interference in the measurement results. 3) We tried to apply Teflon film to the inner walls of the reaction and reference chambers but found that there were some particles produced from the coated wall, which may have been due to bad coating techniques. According to previous studies, particles will take part in the RO_2/HO_2 heterogeneous reactions, thus influencing photochemical O_3 production. Taking these reasons into consideration, we did not coat the inner walls of the reaction and reference chambers with Teflon; instead, we did the photolytic O_3 losses calibration to correct the data, which we think will make our measurement results more accurate.

Table S1: The authors should add standard deviation to average residence times.

Thanks for the suggestions. We have tested in total three sets of experiments at each flow rate, we now added the standard deviation to average residence times in Table S1, we found that for all air flow rates, the standard deviations were <1%, and this may be caused by different operation conditions during the experiments, thus we didn't take this into account when estimate the measured $P(O_3)_{net}$ error, as described in page 17 lines 393-396:

"…the error and LOD of $P(O_3)_{net}$ with a residence time of τ can be calculated using Eq. (7) and Eq. (8), respectively:

$$P(O_3)_{net\_error}=\frac{\sqrt{(O_{X_\gamma})_{rea\_error}^{2}+((9.72\times[(O_X]_{rea\_measured}^{-1.0024})_{rea\_std})^{2}+(O_{X_\gamma})_{ref\_error}^{2}+((9.72\times[(O_X]_{ref\_measured}^{-1.0024})_{ref\_std})^{2}}}{\tau} \quad (7)$$

$$LOD= 3\times P(O_3)_{net\_error} \quad (8)$$"

Fig. S5: The regression lines have non-zero intercepts. These are significant? If so, why? The regression lines for ozone have negative intercepts. In this case, there are large losses of ozone in the high concentration of ozone? For NO_2, how about relative humidity in the experiment? Is there no loss of NO_2 at high relative humidity?

Thanks for the questions, our answers for the different questions are listed as follows:

(1) The regression lines have non-zero intercepts. These are significant? If so, why? The regression lines for ozone have negative intercepts. In this case, there are large losses of ozone in the high concentration of ozone?

The non-zero intercept is not significant. We added the fittings without an intercept and compared the results with those with an intercept. We found that the wall losses of O_3 and NO_2 were not much different, and the wall losses affected by the fitting intercepts for NO_2 and O_3 at an air flow rate of 5 L min^{-1} were all below 4% (as shown in Tables S4 and S5). According to the abovementioned results, we found that when O_3 exhibited negative intercepts, the O_3 wall losses were still below 4 % at ambient O_3 mixing ratios of 0-200 ppb, which was not significant.

We added this explanation in the modified supplementary materials in pages 5-6, lines 73-79:

"The regression lines have non-zero intercepts but not significant. We added the regression fittings without intercept, and compared the regression fitting results with and without intercept (as shown in Figs. S5 and S6). We found that the O_3 and NO_2 wall losses were not much different (as shown in Tables S2 and S3), and the wall loss affected by the fitting intercepts for NO_2 (at ambient mixing ratios of 0-100 ppbv) and O_3 (at ambient mixing ratios of 0-200 ppbv) at the air flow rate of 5 L min^{-1} were all below 4 % (as shown in Tables S4 and S5). We found that when the O_3 have negative intercepts, the O_3 wall losses are still below 4 %, which is not significant."

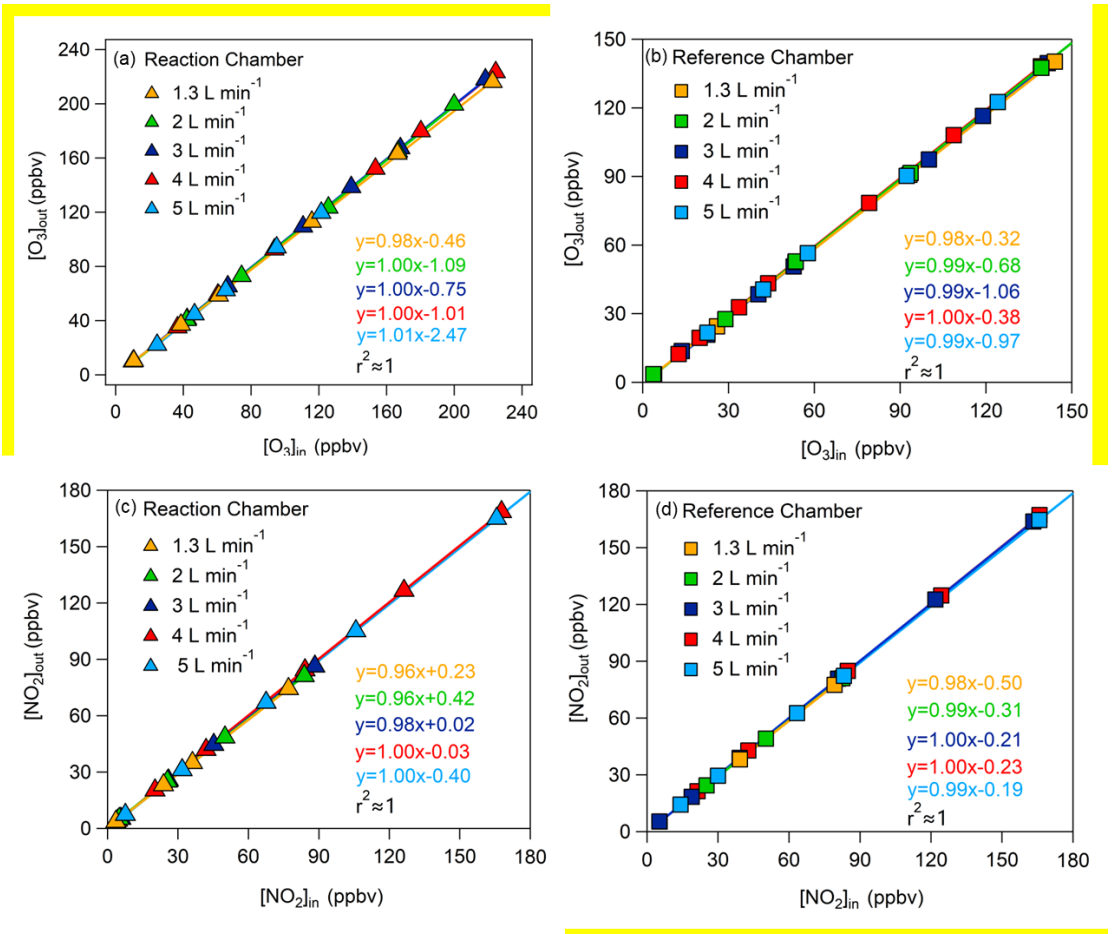

Figure S5: Relationship between (a,b) $[O_3]_{in}$ and $[O_3]_{out}$ and (c,d) $[NO_2]_{in}$ and $[NO_2]_{out}$ in the reaction and reference chambers with intercepts at the flow rates of 1.3, 2, 3, 4, and 5 L min^{-1}, respectively, the solid lines represent the linear fitting of the O_3 or NO_2 mixing ratios at the inlet and outlet of the chambers.

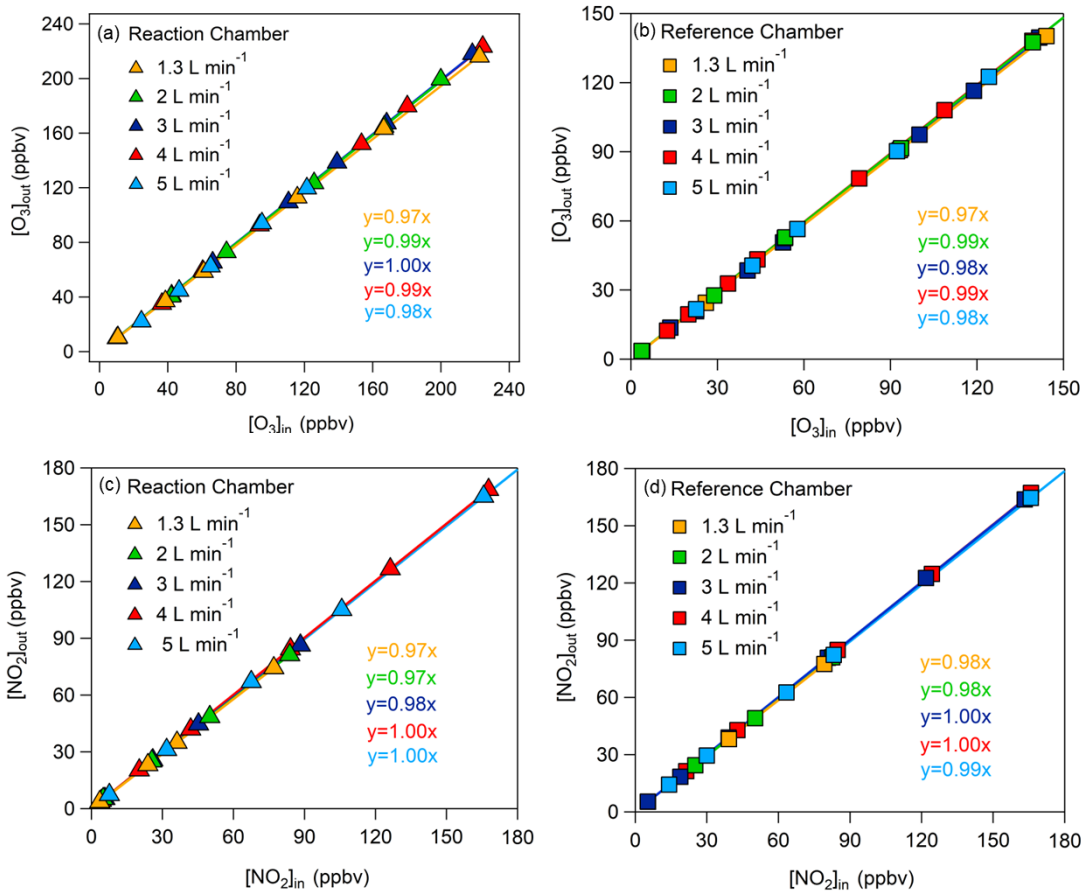

Figure S6: Relationship between (a, b) $[O_3]_{in}$ and $[O_3]_{out}$ and (c,d) $[NO_2]_{in}$ and $[NO_2]_{out}$ in the reaction and reference chambers without intercepts at the flow rates of 1.3, 2, 3, 4, and 5 L min^{-1}, respectively, the solid lines represent the linear fitting of the O_3 or NO_2 mixing ratios at the inlet and outlet of the chambers.

Table S2. Wall losses of O_3 and NO_2 of the reaction and reference chambers with intercepts.

Flow rate of air (L min^{-1})	Wall losses of O_3 (%)		Wall losses of NO_2 (%)	
	Reaction chamber	Reference chamber	Reaction chamber	Reference chamber
1.3	2.0	2.0	4.0	2.0
2	0.0	1.0	4.0	1.0
3	0.0	1.0	2.0	0.0
4	0.0	0.0	0.0	0.0
5	0	0.7	0.3	0.6

Table S3. Wall losses of O_3 and NO_2 of the reaction and reference chambers without intercepts.

Flow rate of air ($L\ min^{-1}$)	Wall losses of O_3 (%)		Wall losses of NO_2 (%)	
	Reaction chamber	Reference chamber	Reaction chamber	Reference chamber
1.3	3.0	3.0	3.0	2.0
2	1.0	1.0	3.0	2.0
3	0.0	2.0	2.0	0.0
4	1.0	1.0	0.0	0.0
5	2.0	2.0	0.0	1.0

Table S4. NO_2 wall loss affected by the intercept.

Ambient NO_2 mixing ratios (ppbv)	Wall loss affected by the intercept (NO_2, %)	
	Reaction chamber	Reference chamber
20	2.0	2.0
40	1.0	1.5
60	0.7	1.3
80	0.5	1.2
100	0.4	1.2

Table S5. O_3 wall loss affected by the intercept.

Ambient O_3 mixing ratios (ppbv)	Wall loss affected by the intercept (O_3, %)	
	Reaction chamber	Reference chamber
50	3.9	2.9
80	2.1	2.2
120	1.1	1.8
160	0.5	1.6
200	0.2	1.5

(2) For NO_2, how about relative humidity in the experiment? Is there no loss of NO_2 at high relative humidity?

We added this explanation in the modified supplementary materials in page 6,

lines 80-87: "Sklaveniti et al. (2018) found that the wall loss of NO_2 is significantly less than that of O_3 at higher humidity levels. However, in our O_3 photo-enhanced uptake experiments, the wall loss of O_3 was almost unaffected by humidity at a flow rate of 5 L min^{-1}. We also tested the wall losses of NO_2 and O_3 in the chamber at a 5 L min^{-1} flow rate at different humidities of 35-75 %, the detailed results are shown in Fig. S7 and S8, which shows that the variation in humidity effected the wall loss of NO_2 and O_3 by 0.03-0.12 % and 1.06-1.19 %, respectively, which is much smaller than the instrument detection error (which is 2 % at ambient NO_2 mixing ratios of 0-100 ppb), thus we didn't count this interference during the data analysis."

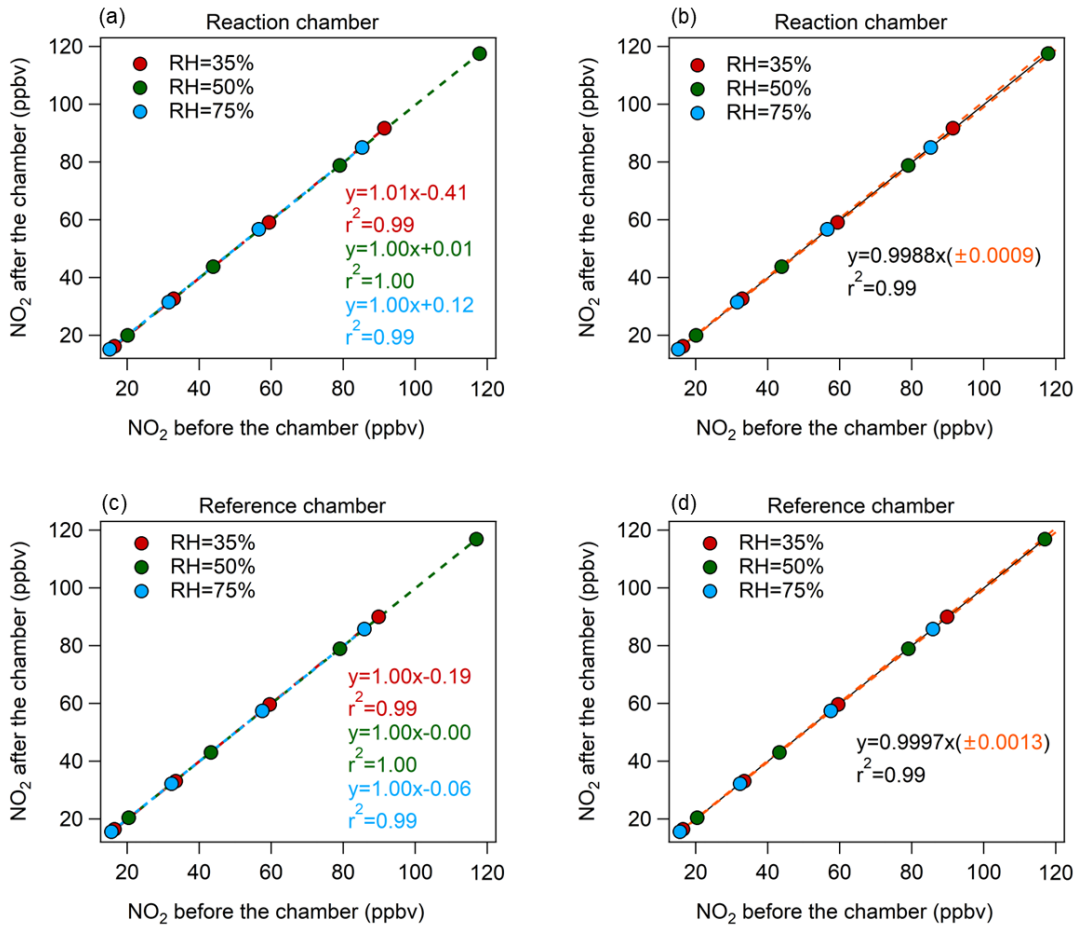

Figure. S7 (a) and (c) represent the NO_2 wall loss at different humidities for the reaction and reference chambers, respectively, (b) and (d) represent the points fitted to all humidities, respectively. Uncertainty in the regression formula was one standard deviation (1σ)."

L218: low → high?

We retained low. We wanted to say the UV film used in this study still has a low light transmission because it could transmit the lights with wavelength>390 nm.

L226: Why the transmittivity of HONO in the reference chamber is lower than that of O_3? How about accuracy and precision of the actinic flux spectrometer?

We measured the transmittivities of all species as follows: we simulated sunlight illumination by adjusting the sunlight (SERIC XG-500B) to provide different intensities of illumination to study the solar UV transmittance through the reaction and reference chambers. The photolysis frequencies of NO_2, O_3, HONO, etc., inside and outside the reaction and reference chambers were measured using an actinic flux spectrometer (PFS-100; Focused Photonics Inc). The results are shown in Table S7.

The actinic flux spectrometer uses a quartz light receiver head to collect solar radiation from all directions and connects the collected light radiation via optical quartz fibers to the spectrometer, which obtains spectral information in a certain wavelength range and transmits the spectrometer data to the industrial control computer. The computer can convert the signal of the spectral scanning into the actinic flux Fλ and calculate the light by integrating the actinic flux with the known absorption cross-section σ(λ) and quantum yield φ(λ). Therefore, there are no differences when measuring the transmittivities of HONO and O_3 on the method and technique aspects. The lower HONO transmittivities in the reference chamber than that of O_3 may be due to the UV protection Ultem film on the reference chamber blocking sunlight with wavelengths < 390 nm, as the spectral atlas of HONO was under 190-395 nm at 298 K (IUPAC, 2004), while the spectral atlas of O_3 was under 410-750 nm at 298 K (IUPAC, 2004). We added this explanation in the modified manuscript on page 11, lines 254-258:

"The reason for the lower HONO transmittivities in the reference chamber than that of O_3 may be that the UV protection Ultem film on the reference chamber blocks sunlight at wavelengths < 390 nm, where the spectral atlas of HONO was under wavelengths of 190-395 nm at 298 K, while that of O_3 was under wavelengths of 410-750 nm at 298 K (IUPAC, 2004, http://iupac. pole-ether.fr/)."

We realized that the transmittivities of HONO in the reference chamber in Baier et al. (2015) was also lower than that of O_3, which demonstrated that our testing results are reasonable. The actinic flux spectrometer has high resolution and sensitivity for actinic flux measurements. There are no deviations or accuracies in the results of the photochemical flux spectrometer, as there are no standards for reference, but the deviation in spectral resolution is ±0.8 nm for the spectral band range (270-790) nm, which is small.

L228: agree → agreement

We changed "agree" to "agreement" in the modified manuscript in line 246.

Table 1: What is Ultem? There are no definitions in the text.

We added the definition of “Ultem” in modified manuscript in lines 128-130 “... an ultraviolet (UV) protection Ultem film (SH2CLAR, 3 M, Japan) was used to cover the outer surface to block sunlight with wavelengths < 390 nm.”

Table 1: The values of 0.019±0.011 should be shaded.

Indeed, we revised it in Table 1.

L272-278 (The airtightness of the reaction and reference chambers): It is hard to follow this section. I think the authors should explain using a schematic diagram for the experiment in the supplement.

Sorry for the confusion description. We have added a schematic diagram for the experiment in the supplementary materials (see Fig. S14), and modified the description accordingly in page13, lines 306-308 in the main manuscript:

“We also checked the airtightness of the reaction and reference chambers by passing through gases with different flow rates based on the schematic diagram shown in Fig. S14

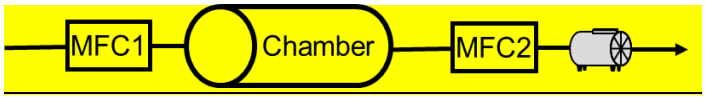

Figure S14. Schematic diagram for investigating the airtightness of the reaction and reference chambers, where MFC1 could measure air flow rate and pressure at the chamber inlet, MFC2 could measure air flow rate and pressure at the chamber outlet.”

L297-L300: For calibration of NO_2, it is not appropriate to perform calibration of NO_2 using a NO_2 standard gas because of low reliability. Calibration should be performed using a gas-phase titration method using NO and O_3.

We apologize for this mistake. We used NO_2 standard gas after we calibrated it using the gas-phase titration method using NO and O_3. We used the CAPS NO_2 monitor reading as a transition value between the two to obtain the NO_2 standard gas and $NO+O_3$ mixing ratios corresponding to the same CAPS NO_2 monitor reading. This result showed that the purification of NO_2 standard gas is sufficient to calibrate the CAPS NO_2 monitor, and we added the related experiments in Fig. S15.

We have added this explanation in the modified supplementary materials in pages 17-18, lines 194-201:

"***Calibration of CAPS NO_2 monitor*** CAPS NO_2 monitor was used to measure the NO_2 standard gas after we have calibrated it using the gas-phase titration method using NO and O_3. We used the CAPS-NO_2 monitor reading as a transition value between the two to obtain the NO_2 standard gas and NO+O_3 mixing ratios corresponding to the same CAPS-NO_2 monitor reading. Results showed the purification of NO_2 standard gas was good enough to calibrate CAPS-NO_2 monitor, as shown in Fig. S15"

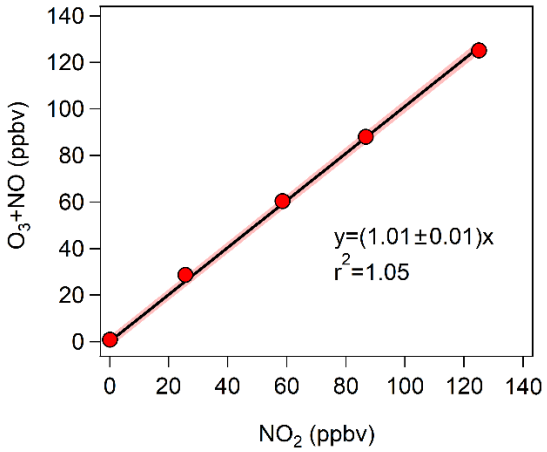

Figure. S15 Correlation between NO_2 standard gas and the NO_2 generated using the gas-phase titration method (NO + O_3).

Reference: The authors should put the list into alphabetical order.

We have revised it in the modified manuscript and supplementary materials.

References

Baier, B. C., Brune, W. H., Lefer, B. L., Miller, D. O., and Martins, D. K.: Direct ozone production rate measurements and their use in assessing ozone source and receptor regions for Houston in 2013, Atmos. Environ., 114, 83-91, http://dx.doi.org/10.1016/j.atmosenv.2015.05.033, 2015.

Cazorla, M., Brune, and W. H.: Measurement of ozone production sensor, Atmos. Meas. Tech., 3, 545-555, https://doi.org/10.5194/amt-3-545-2010, 2010.

Dunlea, E. J., Herndon, S. C., Nelson, D. D., Volkamer, R. M., Martini, F. S., Sheehy, P. M., Zahniser, M. S., Shorter, H., Wormhoudt, J. C., Lamb, B. K., Allwine, E. J., Gaffney, J. S., Marley, N. A., Grutter, M., Marquez, C., Blanco, S., Cardenas, B., Retama, A., Villegas, C. R. R., Kolb, C. E., Molina, L. T., and Molina, M. J.: Evaluation of nitrogen dioxide chemiluminescence monitors in a polluted urban environment, Atmos. Chem. Phys., 7, 2691–2704, https://doi.org/10.5194/acp-7-2691-2007, 2007.

Sadanaga, Y., Kawasaki, S., Tanaka, Y., Kajii, Y., and Bandow, H.: New system for measuring the photochemical ozone production rate in the atmosphere, Environ. Sci. Technol., 51, 2871-2878, https://doi.org/10.1021/acs.est.6b04639, 2017.

Sklaveniti, S., Locoge, N., Stevens, P. S., Wood, E., Kundu, S., and Dusanter, S.: Development of an instrument for direct ozone production rate measurements: measurement reliability and current limitations, Atmos. Meas. Tech., 11, 741-761, https://doi.org/10.5194/amt-11-741-2018, 2018.

Zhou J, Sato K, Bai Y, et al. Kinetics and impacting factors of HO_2 uptake onto submicron atmospheric aerosols during the 2019 Air QUAlity Study (AQUAS) in Yokohama, Japan. Atmos. Chem. Phys., 21, 12243-12260, https://doi.org/10.5194/acp-21-12243-2021,2021.

Zhou J, Fukusaki Y, Murano K, et al. Investigation of HO_2 uptake mechanisms onto multiple-component ambient aerosols collected in summer and winter time in Yokohama, Japan. J. Environ. Sci., 137, 18-29, https://doi.org/10.1016/j.jes.2023.02.030, 2023.

Kotz, J. C., Treichel, P. M., Townsend, J. and Treichel, D.: Chemistry and Chemical Reactivity. 10th 19 ed., Cengage Learning, 2019.